

# Modeling and Feedback Control of Color-tunable LED Lighting Systems

Sina Afshari, Sandipan Mishra, Agung Julius, Fernando Lizarralde, John T. Wen

**Abstract**—This paper presents a color-science-based approach to feedback control design of color-tunable LED lighting systems for smart spaces. The general design problem is posed as the minimization of a cost function consisting of metrics that capture light quality, energy consumption and human comfort. A linear light transport map is used for modeling and identifying the optical fingerprint of the room. The feedback control law is then derived based on the identified model through gradient-based optimization of the cost function. Finally, experimental results are presented to highlight the performance of the feedback control law in terms of (1) energy savings, (2) delivered light quality, (3) adaptivity to external disturbances (such as daylighting) and (4) human comfort.

## I. INTRODUCTION

Lighting contributes to more than 20% of electrical energy consumption in developed countries, costing billions of dollars annually. The need to cut on these expenses along with high quality comfortable light, demands new solutions for everyday lighting purposes. While using Light Emitting Diodes (LEDs) for building lighting has been a topic of interest since LEDs entered everyday applications back in 1970s, today the capabilities brought by solid state lighting together with higher resolution optical data acquisition capability has made LEDs an ideal candidate for lighting of the future.

There have been advances in tackling the lighting control problem using feedback in both non-solid-state and solid state lighting. In non-solid-state lighting the use of photo-sensors by Crisp [1] and Hunt [2], closed loop algorithms by Singhvi et al. [3], wireless sensor networks by Wen et al. [4] and neural networks by Mozer [5] have been explored. In solid state lighting, the compensation of optical and electrical variation of lights by Muthu et al. [6], the effects of dominant wavelength by Zukauskas et al. [7] the use of linear and nonlinear optimization techniques to maximize luminous efficacy and color rendering index in room lighting by Aldrich et al. [8] have been studied.

With the development of cheap optical sensors, closed-loop control holds great promise for lighting in terms of maximizing energy savings while delivering high quality light in the presence of dynamically changing disturbances and model variations. The time-varying nature of the room

Sina Afshari is a graduate student in the Department of Electrical, Systems and Computer Engineering, Sandipan Mishra (mishrs2@rpi.edu) is with the faculty of Mechanical, Aerospace, and Nuclear Engineering. John Wen and Agung Julius are with the faculty of Electrical, Systems and Computer Engineering, Rensselaer Polytechnic Institute, Troy, NY. Fernando Lizarralde is with the faculty of Electronic and Electrical Engineering at the Federal University of Rio de Janeiro, Brazil. This research was supported by the NSF under Smart Lighting Engineering Research Center Contract EEC-0812056 at the Rensselaer Polytechnic Institute.

model and external daylighting, coupled with the nonlinear nature of the human perception of light poses unique control challenges. Thus, there is a need for a systematic formulation of the feedback control design problem of lighting systems for smart spaces. The contributions of this work include (1) a color-science-based approach to modeling, identification and control of lighting systems, (2) a feedback control strategy based on the optical fingerprint of the room, and (3) inclusion of human factors such as comfort in the design methods.

The paper is organized as follows: In section II, the design problem is posed as the minimization of a cost function based on energy consumption and human comfort. In section III, model identification methods together with optimization techniques are used to obtain a feedback control law for LED lighting systems. Finally, in section IV, the results obtained from implementing these algorithms on a lighting testbed are presented and analyzed.

## II. PROBLEM DEFINITION

### A. Problem Formulation

The LED lighting feedback control design problem is defined as determining the LED intensities to maximize light quality and minimize the energy consumption through the use of appropriate metrics subject to constraints that ensure a lighting condition comfortable to the human eye, i.e.,

$$\begin{aligned} \underset{u}{\text{minimize}} \quad & J = \mu_Q(\phi^{des}(\lambda), \phi^\Psi(\lambda, u)) + \alpha \mu_E(u) \\ \text{subject to} \quad & \mathbb{F}(\phi(\lambda, u)) \in \mathbb{S} \end{aligned} \quad (1)$$

where  $\phi^{des}(\lambda)$  is a desired light field,  $\phi^\Psi(\lambda, u)$  is the total lighting condition in the room including the external disturbance (denoted by  $\Psi$ ) as a function of input  $u$ ,  $\mu_Q(\cdot, \cdot)$  is a metric defining the difference in quality of two generated lights,  $\alpha$  is an adjustable weighting coefficient determining the relative cost of light quality compared to desirable energy saving,  $\mu_E(\cdot)$  is a metric of the energy consumed by the LED lighting fixtures,  $\mathbb{F}(\cdot)$  is a function characterizing the comfort of a generated light to the human eye and  $\mathbb{S}$  is the set of all acceptable comfortable lighting conditions.

Here, an arbitrary generated light,  $\phi : \Lambda \rightarrow \mathbb{R}_+ \cup \{0\}$ , is defined as a bounded function such that  $\int_\Lambda |\phi(\lambda)| d\lambda < \infty$ .  $\Lambda$ , the visible light wavelength interval, is defined as  $\Lambda = \{\lambda \in \mathbb{R}_+ \mid \lambda \in [\lambda_l, \lambda_h]\}$ .  $\lambda_l=390$  nm and  $\lambda_h=750$  nm are the lowest and highest wavelengths in the interval respectively [9].  $\phi$  is an infinite dimensional vector representing the power density corresponding to individual wavelengths in the visible light wavelength interval.

The lighting plant in this work is a furnished room with color-tunable LED lighting fixtures on the ceiling, each consisting of red, green and blue (RGB) channels.  $u$  denotes the input to the plant with each of its components determining the intensity of a specific channel of a particular lighting fixture and the light field in the room is the output.

### B. Light Quality Difference Metric, $\mu_Q$

The human eye consists of three types of color sensors: red, green and blue, RGB [10]. Therefore, the light  $\phi(\lambda)$  is sensed by the human eye as a projection on to a three dimensional vector set, the RGB color space, through the corresponding color matching functions  $\{W_R(\lambda), W_G(\lambda), W_B(\lambda)\} \subset \mathbb{W}$ .  $\mathbb{W}$  is defined as  $\mathbb{W} = \{W(\lambda) \mid \forall \lambda \in \Lambda; W(\lambda) \in \mathbb{R}, \int_{\Lambda} |W(\lambda)| d\lambda < \infty\}$ .

In this work, subscript notation is used to specify components of different three dimensional color spaces. The projection operation for an arbitrary pair of light and color matching function,  $\phi(\lambda)$  and  $W(\lambda) \in \mathbb{W}$  is defined as  $\langle \phi(\lambda), W(\lambda) \rangle \triangleq \int_{\Lambda} \phi(\lambda) W(\lambda) d\lambda$ . Assuming an arbitrary generated light  $\phi(\lambda)$ , its projection on the three dimensional RGB vector set,  $\phi_{RGB}$  can be represented as  $\phi_R = \langle \phi(\lambda) W_R(\lambda) \rangle$ ,  $\phi_G = \langle \phi(\lambda), W_G(\lambda) \rangle$ ,  $\phi_B = \langle \phi(\lambda), W_B(\lambda) \rangle$  and  $\phi_{RGB} = [\phi_R \ \phi_G \ \phi_B]^T$ .

The  $\phi_R$ ,  $\phi_G$  and  $\phi_B$  defined above can be negative for some  $\phi(\lambda)$ . In order to avoid the complications caused by this, the XYZ color space was devised by the International Commission on Illumination (*Commission internationale de l'clairage* or CIE) so that the components of the projected vector are always nonnegative. Also  $W_Y(\lambda)$  was chosen identical to the human eye's photopic luminous efficiency function so that the  $\phi_Y$  component of a light in XYZ space is a benchmark of luminance or brightness level of the light. Similarly, the projection of  $\phi(\lambda)$  on XYZ space,  $\phi_{XYZ}$ , is defined as  $\phi_X = \langle \phi(\lambda) W_X(\lambda) \rangle$ ,  $\phi_Y = \langle \phi(\lambda), W_Y(\lambda) \rangle$ ,  $\phi_Z = \langle \phi(\lambda), W_Z(\lambda) \rangle$  and  $\phi_{XYZ} = [\phi_X \ \phi_Y \ \phi_Z]^T$ .

Considering the linearity of the projection operation, there exists a unique linear transformation,  $T$ , that maps the RGB projection of an arbitrary light to its XYZ projection. Thus for arbitrary  $\phi(\lambda)$ ,  $\phi_{XYZ} = T \phi_{RGB}$  and  $\phi_{RGB} = (T)^{-1} \phi_{XYZ}$ .

The xyY color space is another commonly used parametrization to represent the color of a light. The  $x$ ,  $y$  and  $Y$  components in this space are calculated as  $\phi_x = \frac{\phi_X}{\phi_X + \phi_Y + \phi_Z}$ ,  $\phi_y = \frac{\phi_Y}{\phi_X + \phi_Y + \phi_Z}$  and  $\phi_Y = \phi_Y$ .

The set of all achievable  $x$  and  $y$  components in xyY space form the well-known two dimensional chromaticity diagram. The *perceptual nonuniformity* property of the xyY color space makes it an undesirable space to be used in the formulation of the lighting control problem. In a perceptually uniform color space, the Euclidean distance between two arbitrary color points,  $\|\phi_1 - \phi_2\|_2$ , represents how different the corresponding colors  $(\phi_1, \phi_2)$  look to the human eye.

The MacAdam ellipses are defined as ellipses inside which 98% of humans cannot differentiate color. The difference in eccentricity, orientation and size of MacAdam ellipses for different points in the xy plane highlights the lack of perceptual uniformity. This nonuniformity motivated the

community to construct other more uniform color spaces by applying nonlinear transformations on XYZ coordinates such as the  $CIE1976(L^*, a^*, b^*)$  and  $CIE1976(L^*, u^*, v^*)$ .

Although the nonlinearity in the definition of components of the  $CIE1976(L^*, a^*, b^*)$  color space (shortly the Lab color space) adds to the analytical complexity of the problem, its perceptual uniformity is expected to yield a uniform cost function which is essential in order for the mathematical optimal solution to have physical interpretation. Thus the following metric,  $\mu_Q$ , is chosen to characterize the differences in the quality of two lighting conditions

$$\mu_Q(\phi_{des}(\lambda), \phi(\lambda, u)) = \alpha_L \left\| \phi_L^{des} - \phi_L(u) \right\|_2^2 + \alpha_a \left\| \phi_a^{des} - \phi_a(u) \right\|_2^2 + \alpha_b \left\| \phi_b^{des} - \phi_b(u) \right\|_2^2. \quad (2)$$

### C. Energy Consumption Metric, $\mu_E$

For specification of  $\mu_E$ , different norms may be used to indicate the electrical energy consumption as a function of  $u$ . However, typically the input  $u$  is an intensity command delivered to the LED drivers. Therefore, assuming linear efficiency characteristics of the AC/DC converters used in the LED driver circuits and also considering the fact that  $\mu_E$  needs to account for different efficiencies of different channels in the LED lighting fixtures, we propose  $\mu_E(u) = \sum \frac{1}{\eta_i} u_i = \Gamma u$  where  $\eta_i$  is the efficiency of the corresponding channel  $u_i$  in the particular lighting fixture. In this work, we assume  $\Gamma = \begin{bmatrix} \frac{1}{\eta_R} & \frac{1}{\eta_G} & \frac{1}{\eta_B} \end{bmatrix} = \frac{1}{\eta_R} \begin{bmatrix} 1 & 3 & 1 \end{bmatrix}$ .

### D. Human Comfort Function(s), $\mathbb{F}$

There are several characterizations of human comfort from a lighting perspective. The comfort criterion chosen in this work is the Kruithof curve, shown in figure 1, which establishes an acceptable correlated color temperature (CCT) interval for a given (fixed) illuminance level from a human comfort perspective. Considering that each CCT corresponds to a chromaticity point,  $\mathbb{F}$  is chosen as  $\mathbb{F}(\phi(\lambda, u)) = \begin{bmatrix} \phi_x \\ \phi_y \end{bmatrix}$  and  $\mathbb{S}$  is the set of the xy coordinates of the CCTs allowed by the Kruithof curve as comfortable light.

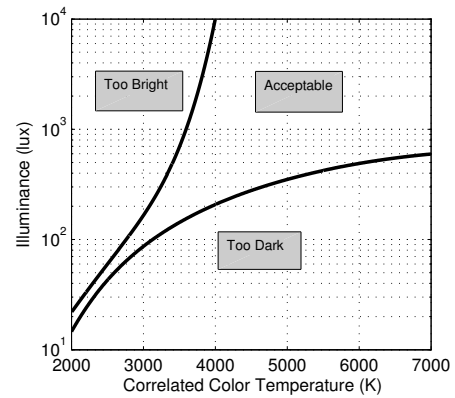


Fig. 1. The Kruithof curve used in this work as a criterion to capture the human comfort factor.

### III. FEEDBACK DESIGN APPROACH

#### A. Model Identification

Previously, the generated light,  $\phi(\lambda, u)$ , was introduced as a function of the input ( $u$ ) to the lighting system. This section presents a framework for modeling this relationship. Considering the vector representation of lighting quantities described in the previous sections, the effect of the generated light on the sensors can be modeled by a linear map called the light transport map [11]. The plant equations in general can thus be written as

$$\begin{cases} \phi = Pu + \psi \\ d = C\phi + v \end{cases} \Rightarrow d = CPu + C\psi + v \quad (3)$$

where  $\phi$  is the generated light,  $u$  is the RGB system input,  $P$  is the map from input to generated light,  $\psi$  is the disturbance spectrum,  $d$  is the RGB sensor readings including different possible types of sensors used,  $C$  is the light transport map and  $v$  is the measurement noise at the sensors. Eliminating the infinite dimensional  $\phi$  from the equations, the new plant model can be described as

$$\begin{cases} d = Au + w + v \\ A = CP \\ w = C\psi \end{cases} \quad (4)$$

with  $A$  being the Light Transport Matrix, or shortly LTM, from the input  $u$  to the sensor measurement  $d$ .  $w$  is the effect of the external disturbance,  $\psi$ , on the sensors. This plant model is used in this work to characterize the input-output relationship for the lighting system. It is important to note that the LTM may be time-varying because of occupancy and room configuration changes.

Several alternate methods can be used for identification of  $A$ , the most conventional one being the least squares. However, following the discussion in the previous section about inconsistency of the 2-norm of RGB data differences with perception of color difference by the human eye, the  $A$  matrix in this work is identified using a nonlinear least squares approach on the 2-norm differences of data in  $CIE1976(L^*, a^*, b^*)$  space. Also the linearity of the model for typical lighting conditions was experimentally verified.

#### B. Feedback Control Law Design

The feedback control design is carried out by applying a gradient-based method to the cost function introduced in (1) using the appropriate metrics, constraints, and models developed above. Particularly two control modes (termed Lab-based and Kruihof-based control) are designed, implemented, and analyzed. The former only considers light quality and energy consumption while the latter also includes constraints for the human comfort factor.

**Lab-based Control:** The objective of this control mode is to optimize the light quality and energy consumption, thus the constraint in (1) is ignored in this case. Therefore, the optimization problem is

$$\begin{aligned} & \underset{u}{\text{minimize}} && J(u) \\ & \text{subject to} && \phi^{meas} = Au + w \end{aligned} \quad (5)$$

where

$$J(u) = \alpha_L \left\| \phi_L^{des} - \phi_L^{meas}(u) \right\|_2^2 + \alpha_a \left\| \phi_a^{des} - \phi_a^{meas}(u) \right\|_2^2 + \alpha_b \left\| \phi_b^{des} - \phi_b^{meas}(u) \right\|_2^2 + \alpha_u \Gamma_u u. \quad (6)$$

The *des* and *meas* superscripts denote the desired and measured lighting conditions respectively and  $\alpha$ 's characterize the weighting of each term in the general cost. Using a gradient-based update method, the control law for the  $k$ -th time-step is given by

$$u_{k+1} = u_k + \varepsilon \left( \begin{bmatrix} \alpha_L^{\frac{1}{2}} \nabla_u(e_L) \\ \alpha_a^{\frac{1}{2}} \nabla_u(e_a) \\ \alpha_b^{\frac{1}{2}} \nabla_u(e_b) \end{bmatrix}^\dagger \begin{bmatrix} \alpha_L^{\frac{1}{2}} (\phi_L^{des} - \phi_L^{meas}) \\ \alpha_a^{\frac{1}{2}} (\phi_a^{des} - \phi_a^{meas}) \\ \alpha_b^{\frac{1}{2}} (\phi_b^{des} - \phi_b^{meas}) \end{bmatrix}_k - \alpha_u \Gamma_u \right) \quad (7)$$

where  $\nabla_u(\cdot)$  is the gradient with respect to  $u$ ,  $\varepsilon$  is a sufficiently small (positive) step size and  $e_L = \phi_L^{des} - \phi_L^{meas}(u)$ ,  $e_a = \phi_a^{des} - \phi_a^{meas}(u)$  and  $e_b = \phi_b^{des} - \phi_b^{meas}(u)$ .

**Kruihof-based Control:** In addition to the control objectives mentioned for Lab-based control, the Kruihof-based controller ensures that the generated lighting condition always stays within the interval of comfortable CCTs. The energy and color quality optimization problem (previously characterized by one cost function in (1)) along with constraints, is approximated in this case as two nested optimization problems given by

$$\begin{aligned} & \underset{(\phi_x^*, \phi_y^*)}{\text{minimize}} && \mu_E(u) \\ & \text{subject to} && (\phi_x^*, \phi_y^*, \phi_L^*) \in \mathbb{S}, \\ & && \phi_L^* = \phi_L^{des} \end{aligned} \quad (8)$$

$$\begin{aligned} & \underset{u}{\text{minimize}} && \mu_Q(\phi^{des}, \phi^{meas}) \\ & \text{subject to} && \phi^{meas} = Au + w. \end{aligned} \quad (9)$$

The optimizer, C1, uses (8) to obtain the chromaticity of the lighting that is the most energy efficient among all the allowable CCTs specified by the Kruihof curve for the desired illuminance  $\phi_L^{des}$ .  $\phi^{des}$  is the lighting condition (in Lab space) corresponding to  $(\phi_x^*, \phi_y^*, \phi_L^*)$ . The second optimizer, C2, determines the input ( $u$ ) to the LED required to generate the lighting condition  $\phi^{des}$ . A schematic of this two-level controller structure is shown in figure 2.

Notice that without disturbance, (8) (or C1) can be solved offline. However, in the presence of disturbance and external lighting the optimal color point must be computed online.

### IV. EXPERIMENTAL RESULTS

#### A. Testbed Description

This section presents a description of the adaptive lighting testbed used to validate the lighting control schemes. There are a total of 12 RGB Renaissance 7" round downlight fixtures with individual control over each channel intensity. The input to each channel is generated on a scale from 0 to 1. The lighting fixtures are located uniformly on the ceiling. Also ten Seachanger wireless color bug sensors distributed

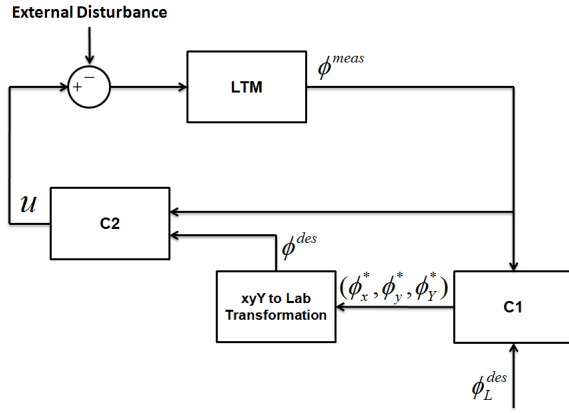


Fig. 2. A schematic diagram of the two-task controller used for the Kruithof-based control.

around the room are used to measure local RGB intensity and illuminance values. These color bugs together with 4 diffused sensor arrays (DSAs, i.e., embedded cameras positioned at the 4 corners of the room) are the sensing devices. In order to avoid privacy violation, the DSA readings are very coarsely pixelized. Figure 3 shows a sample reading compared to the original captured image.

The hardware described previously are connected to a main



Fig. 3. (a) A sample  $15 \times 15$  reading of the diffused sensor array. (b) the corresponding image captured.

server and are capable of transmitting and receiving data with the controller being implemented as a MATLAB code. The interface software governing these connections is Robot Raconteur, a communication library that is compatible with MATLAB, C-sharp and C++ [12].

### B. Lab-based Control

This section presents the experimental results for four tests carried out using the Lab-based controller. In the first experiment, a desired setpoint was chosen and the feedback loop was closed to study the convergence behavior of the plant. In the second experiment, the weighting on the energy term,  $\alpha_u$ , was changed from 0 to 0.04 at the time  $t = 15s$  to illustrate the effect of weighting on energy over the performance. The backlight unit was turned on to simulate an external disturbance at the time  $t = 12s$  in the third experiment to demonstrate the disturbance rejection and energy savings delivered by the controller. Finally, the fourth experiment illustrates the system's performance when both disturbance and weighting on energy are present, starting from  $t = 15s$ .

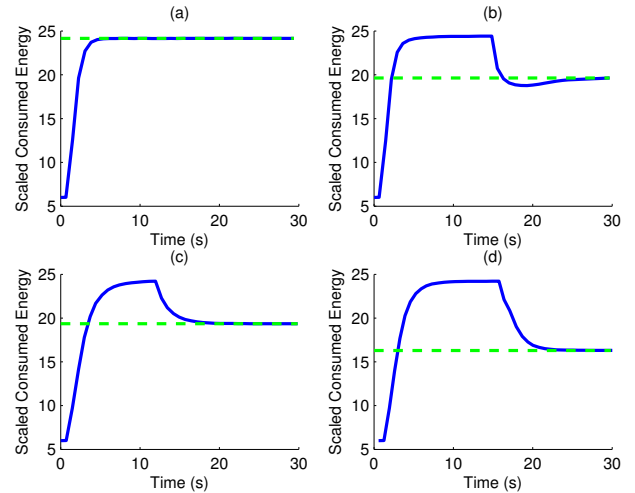


Fig. 4. The scaled energy consumption for different experiments. (a) no disturbance no weighting on energy, (b) no disturbance with weighting on energy, (c) with disturbance no weighting on energy, (d) with disturbance and weighting on energy.

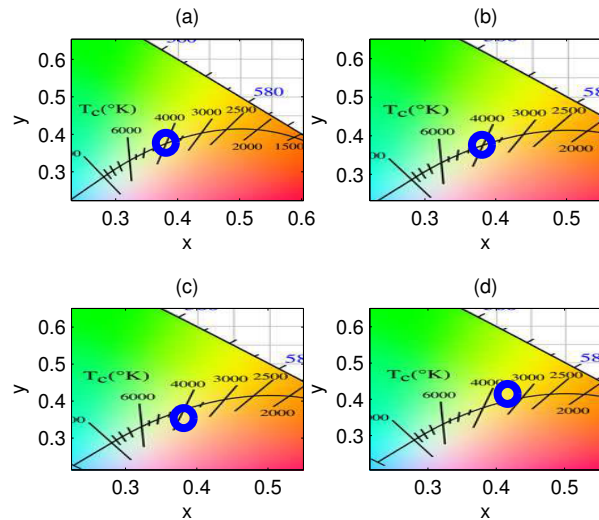


Fig. 5. (a) The desired chromaticity of the generated light, (b) the chromaticity of the generated light for the cases with no disturbance and no weighting on energy, (c) no disturbance and weighting on energy, (d) with disturbance and no weighting on energy.

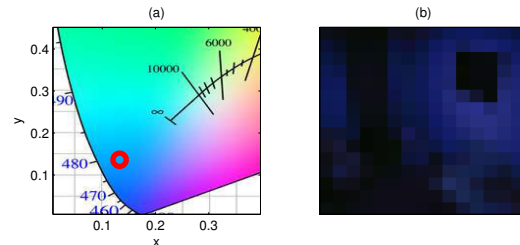


Fig. 6. (a) The chromaticity of the disturbance light. (b) The scaled  $15 \times 15$  pixelated reading of the disturbance.

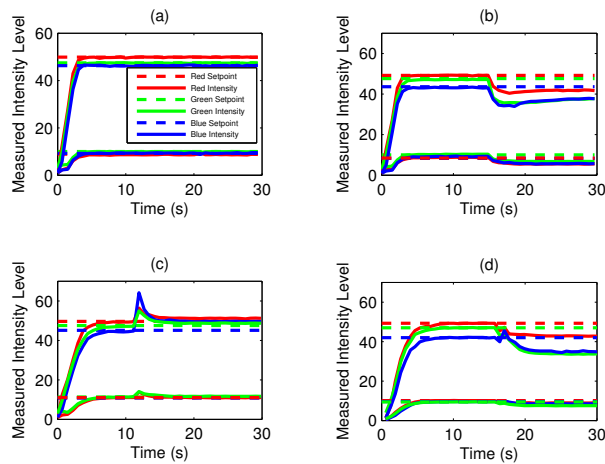


Fig. 7. The convergence of different components of the measured lighting configuration to their setpoints. (a) no disturbance no weighing on energy, (b) no disturbance with weighing on energy, (c) with disturbance no weighing on energy, (d) with disturbance and weighing on energy.

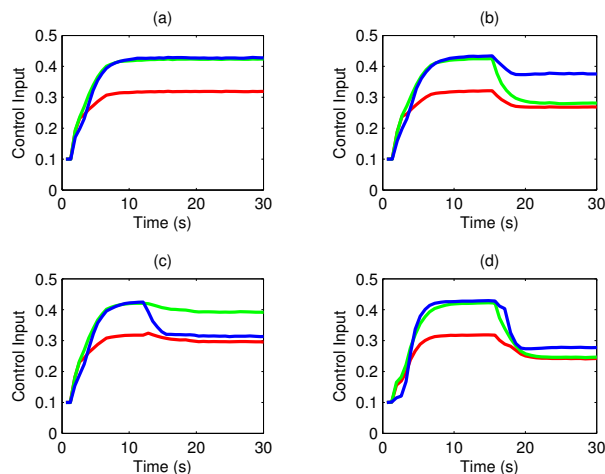


Fig. 8. The control input of the system for different experiments. (a) no disturbance no weighing on energy, (b) no disturbance with weighing on energy, (c) with disturbance no weighing on energy, (d) with disturbance and weighing on energy.

Although extensive human comfort research is required to determine comfortable chromaticity setpoints, here  $CCT = 4000\text{K}$  was chosen as a typical comfortable setpoint. Figures 4 to 8 show the experimental results for the Lab-based control mode. Figure 4 illustrates the energy consumption for the four experiments. It is noteworthy that the saving in  $\alpha_u > 0$  case (second experiment) is obtained by sacrificing the lighting quality by moving away from the chromaticity setpoint, shown in figure 5(c), and decreasing the level of brightness in the room, shown in figure 7(b) and 8(b). The direction of this shift is determined by  $\Gamma_u$ , here moving away from the green part of diagram because of the low efficiency of the green channel of the LEDs. The knob,  $\alpha_u$ , may be set by the user depending on the sensitivity to energy pricing.

In presence of the external disturbance in the third experiment, the energy saving (as shown in figure 4(c)) is obtained because of the utilization of the disturbance as daylighting. Note that the shift observed in figure 5(d) is the controller's reaction to compensate the chromaticity of disturbance (shown in figure 6(a)) resulting in a final lighting condition according to the setpoint. In other words this shift occurs in the **generated light** from LED sources to compensate the effect of disturbance and keep the **total lighting condition** close to the desired condition. The fourth experiment yields the most amount of energy saving, due to both disturbance and weighting on energy.

Thus, the Lab-based controller achieves two objectives: (1) through the tuning knob  $\alpha_u$  the controller trades off matching the desired lighting condition against energy savings, and (2) the Lab controller compensates the presence of an external disturbance and utilizes it as daylighting to save energy.

### C. Kruithof-based Control Mode

For the Kruithof-based controller, human comfort plays a critical role in determining allowable set-points. Two experiments were carried out to demonstrate the performance of the controller in the absence and presence of external disturbance (daylight). The level of illuminance in these experiments was first set to 400lux for which the Kruithof curve predicts an acceptable CCT interval approximately from 3500K to 5500K. The external disturbance was chosen as before. Figure 9 shows that, for the no-disturbance case,

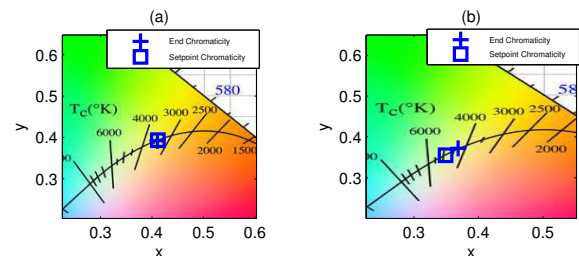


Fig. 9. The desired chromaticity of the generated light compared to that of the setpoint for the two experiments, (a) without disturbance and (b) with disturbance.

the most energy efficient CCT is 3500K. However, in the case with disturbance, 4900K is determined as the most energy efficient CCT. The optimal CCT is clearly dependent on the spectral content of external disturbance coming in. For example, with more blue in the external disturbance, the most energy efficient CCT tends to move to higher temperatures which have more blue content.

Figures 10(a) and (b) show the electrical energy consumptions in the two experiments with respect to time. We note that the energy consumption is lower when the disturbance is present, because part of the disturbance is exploited for illumination. Therefore, the Kruithof based controller can achieve an energy saving of 10% while guaranteeing that the human comfort condition is still satisfied. Figures 10(c) and (d) show the relative cost of generation for lights with different CCTs in each case. Note that the points which

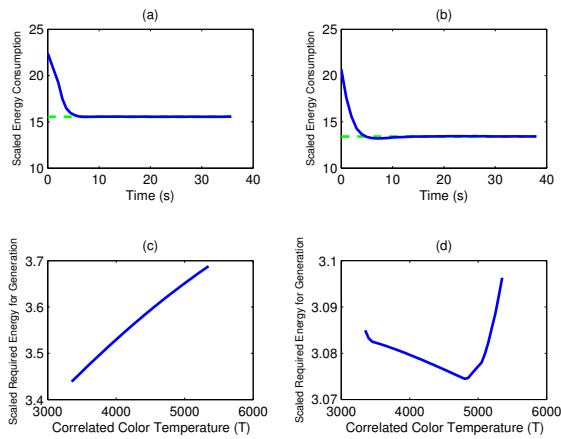


Fig. 10. The scaled energy consumption for the two experiments, (a) without disturbance and (b) with disturbance. The required energy for generation of the light with different CCTs for the two experiments, (c) without disturbance and (d) with disturbance.

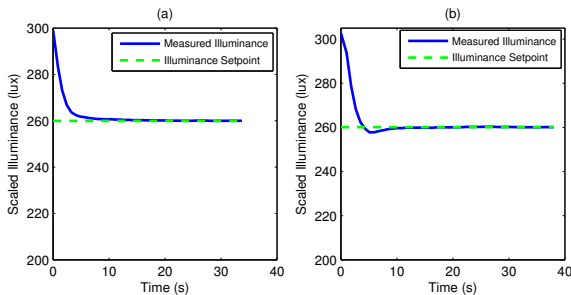


Fig. 11. The convergence of the illuminance level to its setpoint in the two experiments, (a) without disturbance and (b) with disturbance.

yield the minimum for the functions plotted in figure 10(c) and (d) determine the corresponding CCT setpoints 3500K and 4900K (and therefore the chromaticity set points) for the two experiments, respectively. Figure 11 illustrates the performance of the brightness control loop (C2) of the controller in this mode in no-disturbance and with disturbance configurations respectively.

Thus, the Kruithof-based controller achieves two objectives: (1) it ensures that the human comfort factor is always guaranteed while maximizing energy savings, and (2) it compensates the presence of an external disturbance and utilizes it as daylighting to save energy.

## V. CONCLUSION AND FUTURE WORK

In this paper a systematic approach to the problem of modeling and feedback control for color-tunable LED lighting systems was presented, the required techniques and algorithms were discussed and implemented and the results were analyzed. These results are applicable to demand-based lighting control to yield even more significant energy saving. The key conclusions from this research are:

- By appropriate choice of cost function based on color scientific metrics, the trade-off between quality of light

and energy consumption for LED lighting systems can be governed.

- Disturbance light (daylight) can be utilized for lighting purposes, reducing the energy consumption by up to 20% while maintaining the quality of lighting.
- Human comfort factor must also be included in LED lighting control systems, ensuring generation of comfortable light.

Several extensions of the research presented in this paper are possible. Online adaptive estimation of the light transport matrix in parallel with the control process is expected to yield a smarter controller due to the time-varying nature of the lighting plant. Also the development of distributed algorithms in both sensing and control fronts such as leader-follower structures is promising in terms of smart control of lighting systems. These future research avenues are currently being pursued by the authors.

## VI. ACKNOWLEDGMENTS

The authors gratefully acknowledge the contribution of John Wason, graduate student, Prof. Arthur Sanderson and Prof. Robert Karliceck, from the Smart Lighting ERC.

## REFERENCES

- [1] V. Crisp, "Preliminary study of automatic daylight control of artificial lighting," *Lighting Research and Technology*, vol. 9, no. 1, pp. 31–41, 1977. [Online]. Available: <http://lrt.sagepub.com/content/9/1/31.abstract>
- [2] D. Hunt, "Simple expressions for predicting energy savings from photo-electric control of lighting," *Lighting Research and Technology*, vol. 9, no. 2, pp. 93–102, 1977. [Online]. Available: <http://lrt.sagepub.com/content/9/2/93.abstract>
- [3] V. Singhvi, A. Krause, C. Guestrin, J. H. Garrett, Jr., and H. S. Matthews, "Intelligent light control using sensor networks," in *Proceedings of the 3rd international conference on Embedded networked sensor systems*, ser. SenSys '05. New York, NY, USA: ACM, 2005, pp. 218–229. [Online]. Available: <http://doi.acm.org/10.1145/1098918.1098942>
- [4] Y.-J. Wen, J. Granderson, and A. M. Agogino, "Towards embedded wireless-networked intelligent daylighting systems for commercial buildings," *Sensor Networks, Ubiquitous, and Trustworthy Computing, International Conference on*, vol. 1, pp. 326–331, 2006.
- [5] M. Mozer, "The neural network house: An environment that adapts to its inhabitants," *Proceedings of the American Association for Artificial Intelligence*, 1998.
- [6] S. Muthu, F. Schuurmans, and M. Pashley, "Red, green, and blue led based white light generation: issues and control," in *Industry Applications Conference, 2002. 37th IAS Annual Meeting. Conference Record of the*, vol. 1, 2002, pp. 327 – 333 vol.1.
- [7] A. Zukauskas, R. Vaicekaskas, F. Ivanauskas, R. Gaska, and M. S. Shur, "Optimization of white polychromatic semiconductor lamps," *Applied Physics Letters*, vol. 80, no. 2, pp. 234 –236, jan 2002.
- [8] M. Aldrich, N. Zhao, and J. Paradiso, "Energy efficient control of polychromatic solid state lighting using a sensor network," in *Society of Photo-Optical Instrumentation Engineers (SPIE) Conference Series*, ser. Society of Photo-Optical Instrumentation Engineers (SPIE) Conference Series, vol. 7784, Aug. 2010.
- [9] C. Starr, C. A. Evers, and L. Starr, *BIOLOGY: CONCEPTS AND APPLICATIONS*, 8th ed.
- [10] G. Wyszecki and W. S. Stiles, *Color science: concepts and methods, quantitative data, and formulae*, 2nd ed.
- [11] P. Sen and S. Darabi, "Compressive dual photography," *Computer Graphics Forum*, vol. 28, no. 2, pp. 609–618, 2009. [Online]. Available: <http://dx.doi.org/10.1111/j.1467-8659.2009.01401.x>
- [12] J. Wason and J. Wen, "Robot Raconteur: A Communication Architecture and Library for Robotic and Automation Systems," in *IEEE International Conference on Automation Science and Engineering*, 2011.